International Journal of Electrical and Electronics Engineers
Vol. No.8 Issue 02, July-December 2016
ISSN (O) 2321-2055
ISSN (P) 2321 -2045

DESIGN OF HYBRID DC/DC STEP-UP CONVERTER WITH HIGH VOLTAGE GAIN FOR FUEL CELL BASED ELECTRIC VEHICLE APPLICATIONS

Hemanth Kumar Karri[1], Siva Kumar S V Jagarapu[2]

[1,2]Department of Electrical & Electronics Engineering, GMR Institute of Technology Rajam, Srikakulam District, AP, (India)

ABSTRACT

The consumption of fossil fuels leads to increases environmental degradation. This will increase demand for hydrogen fuel cell technology. However, the voltage produced from this source is less therefore it requires boost converter which steps up the low voltage to high voltage for electric vehicle applications. This paper introduces the hybrid boost converter with high voltage gain which is extracted from single phase diode clamped three level inverter. The present converter is non isolated type, which means no EMI problems. In addition to this the voltage across the power switches will be half of the output voltage, which minimizes converter peak current, ripple content in the output voltage with the help of inductor and switched capacitors. The effectiveness of present converter is observed with MATLAB/Simulink platform. Finally, the obtained results are discussed.

Key words- Boost Converter, Dc Battery, Diode Clamped Inverter, Electric Vehicle, Hydrogen Fuel Cell, Non-Isolated, Voltage Gain.

I. INTRODUCTION

In the recent trend, the usage of renewable resources is more than fossil fuels because of environmental pollution issues. By utilizing renewable energy sources, we can generate electricity easily for power the electrical loads. In this way, the generating electricity is low from available sources i.e., solar, wind and fuel cell technologies. In the recent scenario, the automobile industries are fully depends on fossil fuels for combustion of engines. However, thermal vehicles are responsible for high emission of carbon content into the atmosphere. To maintain zero emissions of carbon in the form of smoke, we have to change the situation to utilizing of renewable sources. In these, the fuel cell technology is more comfortable for generating electricity. But the production of voltage from this technology is low, so it requires step up conversion system which boosts the low voltage to high voltage for vehicle propulsion. This paper introduces three level hybrid dc-dc boost converter for fuel cell based electric vehicle [1]. According to fuel cell source, output voltage of single cell is not sufficient to drive the vehicle. For this reason, we have to connect in series and parallel with each other to obtain high level dc voltage. But, the performance of the fuel cell may get collapsed. Therefore to improve the performance of this technology with a hybrid dc-dc boost converter with high voltage gain shown in Fig.1. This converter boosts the low voltages (40-68 V) to high voltages (300-600 V) [2]. The main features of this converter are high transfer gain with low duty ratio and high efficiency. However, the designing of classical boost converters with

International Journal of Electrical and Electronics Engineers
Vol. No.8 Issue 02, July-December 2016
ISSN (O) 2321-2055
ISSN (P) 2321 -2045

high duty ratio because of electromagnetic interference, reverse recovery and efficiency problems. According to the classification of boost converters, we have isolated and non-isolated type of converters. Isolated type converters having transformer to eliminate dc path between input and output sides by changing of turns ratio with high voltage gain [3]. But, the isolated boost converters have a leakage inductor, which affects the performance of converter like voltage stress on power switches and electromagnetic interference. To minimize these affects various converter structures have been implemented with high lift technique, but this leads to conduction loss. So, there is no best solution for extinguish the voltage stresses on the power switches with classical converters.

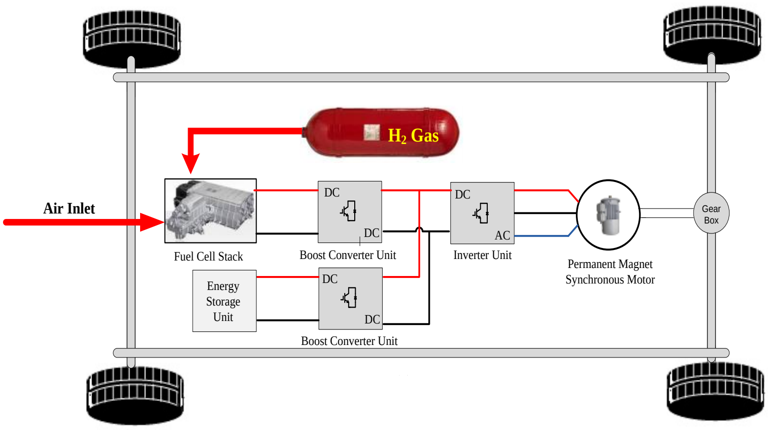

Figure 1. Block Diagram of the Fuel Cell Electric Vehicle

This paper introduces three level boost converter for fuel cell applications to minimize the voltage stress and conduction loss by maintaining high voltage gain [4]. From the literature survey, this type of technique is derived from three level diode clamped inverter and is explained in the analysis of converter design. The duty cycle of this converter is operated nearer to 0.5 with high step-up gain. Therefore, in Section II, design of PEM fuel cell is presented and analyzed; the analysis of three level hybrid topology in Section III; Section IV presents the operation of three level boost converter; converter design is explained in Section V; Section VI presents a discussion about the obtained results; finally, the conclusion is carried out in Section VII.

II. DESIGN OF PEM FUEL CELL

In the recent scenario, the application of fuel cell technology is the best source than other renewable sources. It is electro chemical device, which converts chemical energy into electrical energy. According to operation of fuel cell stack, the electric energy produces when hydrogen gas is chemically reacts with atmospheric air [5]. In this era, Proton Exchange Membrane Fuel Cells are well suited for electricity generation. The PEMFC stack has an advantage that it can operate under low temperatures [6].

Reaction at anode and cathode is given by,

$$2H_2 = 4H^+ + 4e^- \tag{1}$$

$$O_2 + 4H^+ + 4e^- = 2H_2O \tag{2}$$

Over all electrochemical reaction is given by,

International Journal of Electrical and Electronics Engineers
Vol. No.8 Issue 02, July-December 2016
ISSN (O) 2321-2055
ISSN (P) 2321 -2045

$$H_2 + \frac{1}{2} O_2 = H_2O + \text{ElectricalEnergy} + \text{Heat} \tag{3}$$

According to the Fig. 2 shown, the fuel cell stack output voltage is expressed in equation, where E_{nerst} is the thermodynamic potential of the fuel cell, V_{act} is the activation voltage drop, V_{ohmic} is the ohmic losses due to internal resistance, V_{con} is the voltage drop due to the concentrations.

In general, the output power of the fuel cell stack is high when the output voltage is high. The fuel cell stack consists a solid polymer as dielectric membrane for ion exchanging in between anode and cathode electrodes. But, the group of ions are stagnated on the surface of electrolyte due to this there is no chance to conduction. For conduction of current is possible by external arrangement between two electrodes [7].

$$E_{Nerst} = 1.229 - 0.85 \times 10^{-3} (T - 298.15) + 4.308 \times 10^{-5} \times T \times [\ln(P_{H_2}) + \frac{1}{2} \ln(P_{O_2})] \tag{4}$$

$$V_{act} = -[\zeta_1 + \zeta_2 \times T + \zeta_3 \times T \times \ln(C_{O_2}) + \zeta_4 \times T \times \ln(I_{FC})] \tag{5}$$

Where T is the temperature of fuel cell in Kelvin, P_{H2} and P_{O2} represents the pressures of hydrogen and oxygen in atmospheres. I_{FC} is fuel cell current and ζ_i is the parametric coefficients are discussed in [8].

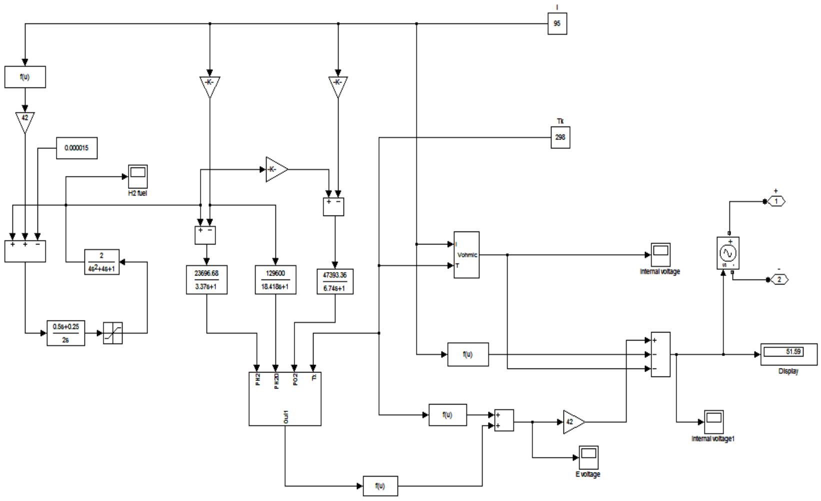

Figure 2. Overall model of fuel cell stack

The equation for calculating of concentration of oxygen C_{O2} is

$$C_{O_2} = \frac{P_{O_2}}{5.08 \times 10^6 \exp\left(\frac{-498}{T}\right)} \tag{6}$$

Fuel cell's ohmic voltage and concentration voltage are expressed as

$$V_{ohmic} = I_{FC} \times (R_{el} + R_P) \tag{7}$$

$$V_{ohmic} = -\beta_0 \times \ln\left(1 - \frac{I_d}{I_{max}}\right) \tag{8}$$

Where R_{el} is the resistance of electron flow, J_d is the current density and β_O is the constant parameter.

The parameter R_p is expressed as proton's flow equivalent resistance,

$$R_P = \frac{\rho_m}{A_r} \times L \tag{9}$$

International Journal of Electrical and Electronics Engineers
Vol. No.8 Issue 02, July-December 2016
ISSN (O) 2321-2055
ISSN (P) 2321 -2045

Where L is the width of polymer membrane, A_r is the active cell area and ρ_m is the specific resistivity of the membrane expressed as

$$r_m = \frac{181.6\times\left[1+0.03\times\left(\frac{I_{FC}}{A_r}\right)+0.62\times\left(\frac{T}{303}\right)^2\times\left(\frac{I_{FC}}{A_r}\right)^{2.5}\right]}{\left[\lambda-0.63-3\times\left(\frac{I_{FC}}{A_r}\right)\exp\left(4.18\times\left(\frac{T-303}{T}\right)\right)\right]} \quad (10)$$

$$V_{FC} = E_{Nerst} - V_{Ohmic} - V_{Actual} - V_{Conc} \quad (11)$$

III. ANALYSIS OF THREE LEVEL HYBRID TOPOLOGY

From the analysis of three level diode clamped inverter, two dc-dc converters (buck & boost) are extracted. Here, four power switches (Q_1-Q_4) with diodes (D_1-D_4) which are connected in anti parallel to each other for step-up and step-down of the voltage level. Based on this topology, two more boost three level converters are extracted [9]. These two converters does not having any command on voltages across the capacitors ($C^1{}_1$, $C^2{}_1$) and ($C^1{}_2$, $C^2{}_2$), when these can be operated separately.

The principal of operation was discussed in [5], to improve the gain and efficiency of the converter. Generally, the starting torque is high for electrical vehicle propulsion. This will leads to two deduced boost converters are synthesized based on the single phase diode clamped inverter with two three level legs is explained [10]. Furthermore, the input side power level is increasing with the help of series connection of input side voltages 'V_{in1}' and 'V_{in2}'. The output power level of the converter can be improved by making parallel connection of two output resistors. The capacitors namely, ($C^1{}_1$ & $C^2{}_1$) and ($C^1{}_2$ & $C^2{}_2$) can be connected in parallel, then equivalent to C_1 and C_2 explained in [11]. The load resistors R_1 and R_2 are equal to R_L and boost inductors L_1 and L_2 are equal to L. Based on the analysis of three level hybrid boost technique, next going to be explaining the operation of suggested topology and gating control of power switches with the pulse width modulation (PWM) technique [12].

IV. OPERATION OF THREE LEVEL BOOST CONVERTER

4.1. Conduction States of Topology

According to the Figure 3, the output voltage is achieved by the following equation

$$V_{ab} = V_{ag} - V_{bg} \quad (12)$$

Where V_{ag} and V_{bg} are the voltages of two half bridges and V_o be the output voltage of the boost converter. This voltage can be achieved by using filtering capacitors C_1 and C_2. Coming to the storage elements, inductor and capacitors are playing vital role in the converter design.

When the thyristors $Q_1 - Q_4$ are switched off, then the capacitors C_1 and C_2 are in series and charged together by input voltage V_{in} and energy stored boost inductor L through diodes $D_1 - D_4$. Then the output voltage V_o is equal to V_{ab}. When the thyristor Q_4 is switched on, then C_1 is charged by input voltage V_{in} and energy through diodes D_2, D_1 and D_{Q3} transferred from the boost inductor shown in Fig.3. In the moment, C_2 is discharged through load resistor and the output voltage is observed as $V_o/2$, which is appeared across the capacitor C_1 [4].

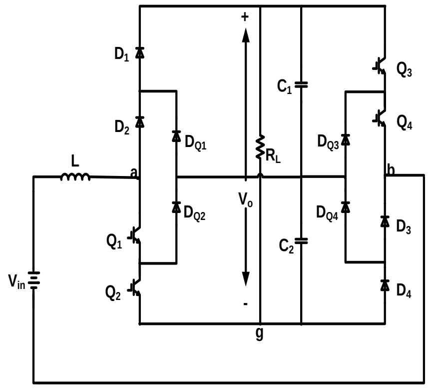

Figure 3. High Gain Boost Converter

And, the instantaneous voltage $V_{ab} = V_o/2$ is appeared across the C_2 is charged by input voltage V_{in} and energy transformed from the inductor L through diodes D_{Q2}, D_4 and D_3, when Q_1 is switched on and energy is discharged from the C_1 to load. When both the thyristors Q_1 and Q_2 are turned on, the energy stored in inductor L through diodes D_4 and D_3. Meanwhile, the capacitors C_1 and C_2 are discharged together for the load.

4.2. Switching Control for Power Switches of Topology

According to the operation of present converter, the switches Q1-Q4 are controlled by PWM control. The balancing capacitors are going to charging and discharging modes are based on the decision of power switches with respect to triggering time. The phase to ground voltages V_{ag} and V_{bg} for both half bridges are expressed as

$$V_{ab} = (1 - S_1 \times S_2)\ (V_{c1} + V_{c2}) - (S_1 - S_2) \times V_{c1} \quad (13)$$

$$V_{bg} = S_3 \times V_{c1} + S_4 \times V_{c2} \quad (14)$$

Where S_1, S_2, S_3, S_4 are the function of the switching states. By equating 1, 2 & 3 equations and V_{ab} is derived as

$$V_{ab} = \left[(1 - S_1)\ (1 + S_2) - S_3\right] \times V_{c1} + (1 - S_1 \times S_2 - S_4) \times V_{c2} \quad (15)$$

From the figure, the term modulation index is defined as the ratio of amplitude of modulation wave and amplitude of carrier wave. Here, two modulation indices m_a and m_b are used to modulate the carrier signals Carrier_ 1 and Carrier_2 are provided with 180^0 phase shifted to required level and leads to decide the turn on and turn off times of power switches. PWM control technique can be described as,

$$m_b > V_{carrier\_1},\ S_1 = 0;\ m_a < V_{carrier\_2},\ S_2 = 0;\ m_a < V_{carrier\_1},\ S_3 = 0;\ m_b > V_{carrier\_2},\ S_4 = 0.$$

According to the figure 5, the current through the inductor & voltage across two capacitors are follows the switching times for charging & discharging purpose. Let us consider, the dynamic behaviour of capacitors is explained as, the capacitors C_1 & C_2 are in charging mode at initial conditions.

According to the Figure 4 shown, the modulated wave is compared with carrier signal can be achieved switching states of the power switches Q_1-Q_4 [4].

International Journal of Electrical and Electronics Engineers
Vol. No.8 Issue 02, July-December 2016
ISSN (O) 2321-2055
ISSN (P) 2321 -2045

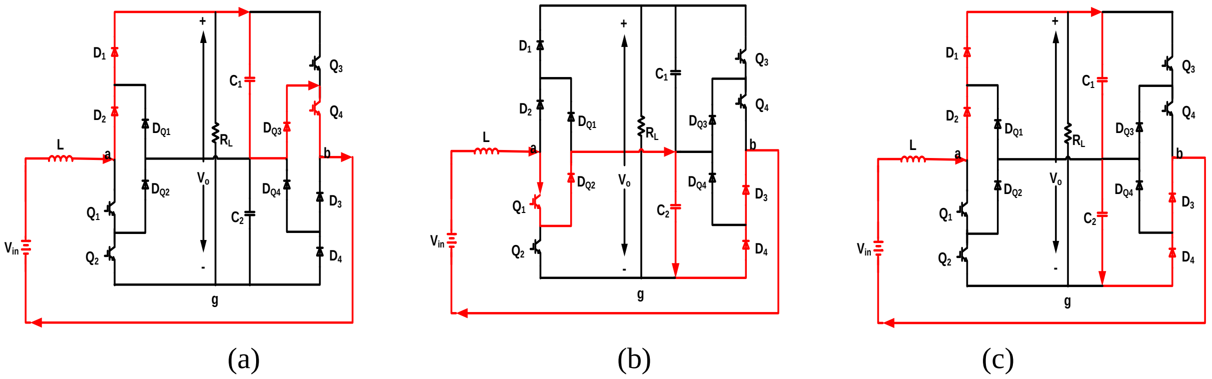

Figure 4. Operation states of suggested Converter. (a) D_1, D_2, Q_4, D_{Q3} = ON and $V_{ab} = V_o/2 = V_{C1}$; (b) Q_1, D_{Q2}, D_3, D_4 = ON and $V_{ab} = V_o/2 = V_{C2}$; (c) D_1, D_2, D_3, D_4 = ON and $V_{ab} = V_o = V_{C1}+V_{C2}$

If the switch Q_1 is ON, then the capacitor C_1 is enters into discharging mode but the capacitor C_2 is remains in charging mode. After small instant of time, Q_2 is comes to turn on position, it leads to both capacitors are going for discharging mode. Like this, the voltage across the two capacitors is half of the output voltage and they are balanced for uninterrupted operation of power converter and the corresponding voltage is $V_{ag} = V_o/2$, $V_{bg} = 0$. Alternatively, the states are changing with respect to modulated indices. The charging and discharging time of capacitors are mentioned below,

$$t_1 = t_2 = \frac{t_{on1} - t_{on2}}{2} \tag{16}$$

$$t_3 = t_4 = \frac{t_{on4} - t_{on3}}{2} \tag{17}$$

Here, t_1-t_4 is represented as discharging and charging times of capacitors C_1 and C_2. The discharging time of C_1 is $(t_1 + t_2)$ and for C_2 is $(t_3 + t_4)$ [12].

4.3. High Step-up Technique for Boost Converter

Based on the conduction path of present converter, the energy is stored and transferred in inductor when $V_{ab} = 0$ & $V_{ab} = V_o$ or $V_o / 2$ respectively.

The following equations are derived in one time period,

$$W_{st} = V_{in} \times I_L \times t_{on2} \times 2 \tag{18}$$

$$W_{tr} = \left(V_o - V_{in}\right) \times I_L \times \left(T/2 - t_{on1}\right) \times 2 + \left(V_o/2 - V_{in}\right) \times I_L \times \left(t_1 + t_2\right) \times 2 \tag{19}$$

$$W_{st} = W_{tr} \tag{20}$$

From the above energy equations, the output of three level boost converter is given as,

$$V_o = \frac{V_{in}}{1-(d_1+d_2)} \tag{21}$$

According to the output equation, the modulated index is written as

$$M = \frac{1}{m_b - m_a} = \frac{V_0}{V_{in}} \tag{22}$$

From above equation, if modulation indices m_b and m_a are closer to one, then voltage gain will be high. The equations are derived for modulated indices will be,

$$m_a = 0.5 - \frac{3}{4M} \quad (23) \qquad m_b = 0.5 + \frac{1}{4M} \quad (24)$$

V. CONVERTER DESIGN

The design of suggested converter is discussed in this section. The following parameters are required to be designed for converter.

5.1. Boost Inductor

The boost inductor is plays very important role for step up the low voltage. The most critical parameter for calculation of inductor is the saturation current. If the saturation current of the inductor is less than the converter required peak current, then the converter will not support for conduction [13].

$$L = \frac{V_{in} \times (V_o - V_{in}) \times T_s}{2 \times \Delta i_L \times V_o} \quad (25)$$

5.2. Voltage Gain

According to volt-sec balance on inductor, $M = \frac{V_0}{V_{in}}$ (26)

When parasitic resistance of inductor and source resistance are considered, so the equation can be expressed as

$$V_0 = \frac{V_{in}}{1-(d_1+d_2)} \left\{ \frac{1}{1+\left(\frac{\alpha}{1-(d_1+d_2)} \right)} \right\} \quad (27)$$

Where, $\alpha = \frac{R_1+R_2}{R}$ (28)

5.3. Current Ripple

In each sub-cycle, the change of current with respect to time is constant. Consider duty ratio as nearer to 0.5. The sub-period is dT_s and (1- d) Ts

$$\Delta i = \frac{(d_1+d_2) \times (1-(d_1+d_2)) \times R \times T_s}{L} \quad (29)$$

5.4. Voltage Ripple

The ripple in voltage is appeared due to charging and discharging modes of the capacitor [14]. The ripple voltage is approximately equals to

$$\Delta v = \frac{I_0 \times (d_1+d_2) \times T_s}{C} \quad (30)$$

International Journal of Electrical and Electronics Engineers
Vol. No.8 Issue 02, July-December 2016
ISSN (O) 2321-2055
ISSN (P) 2321 -2045

VI. RESULTS AND DISCUSSIONS

The present converter is simulated in MATLAB/Simulink platform and the inverter current in steady state with respect to gating signals are shown in figure. Here, the fuel cell stack is acting as input source for presented converter. The filtering capacitors are balanced through the load resistor is varied with respect to time. From the shown Fig. 5, the voltage produced by the fuel cell is 51.68V at 0.1 sec.

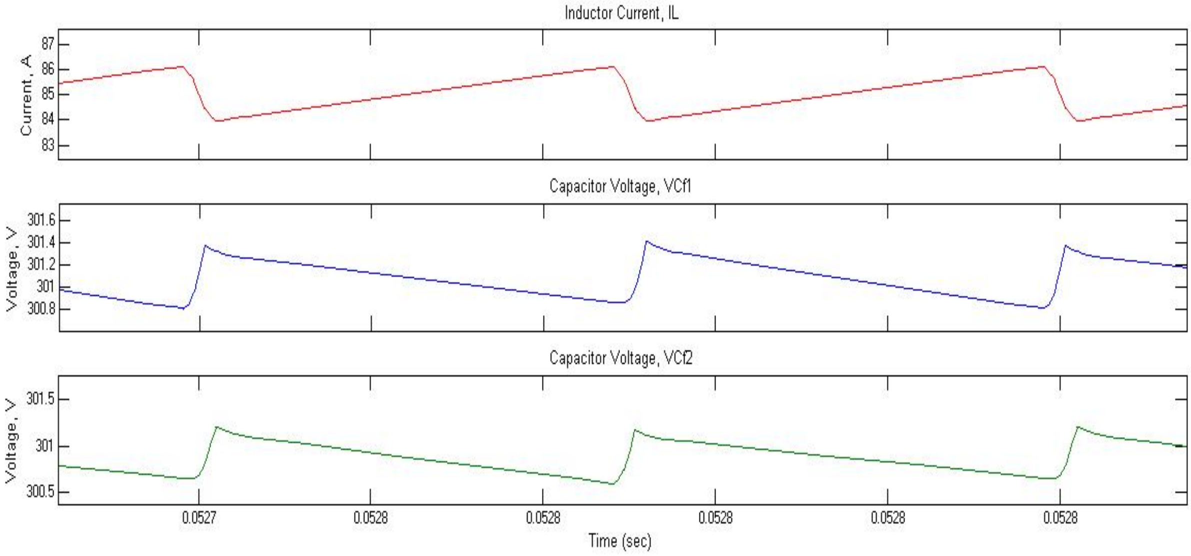

Figure 5. Steady state inductor current and voltage across filtering capacitors

According to the pressures of hydrogen and oxygen, the PEM fuel cell stack voltage is about 51.68 V for starting current is considered as 20A at 0.08 sec is shown in Fig.6 at temperature of 25^0 C (298^0 K).

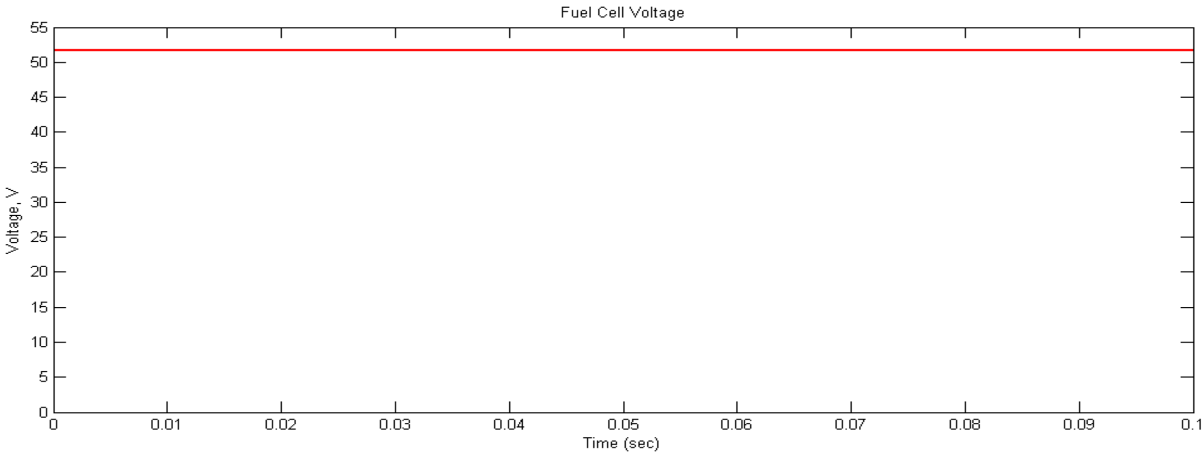

Figure 6. Fuel cell stack output voltage

International Journal of Electrical and Electronics Engineers
Vol. No.8 Issue 02, July-December 2016
ISSN (O) 2321-2055
ISSN (P) 2321 -2045

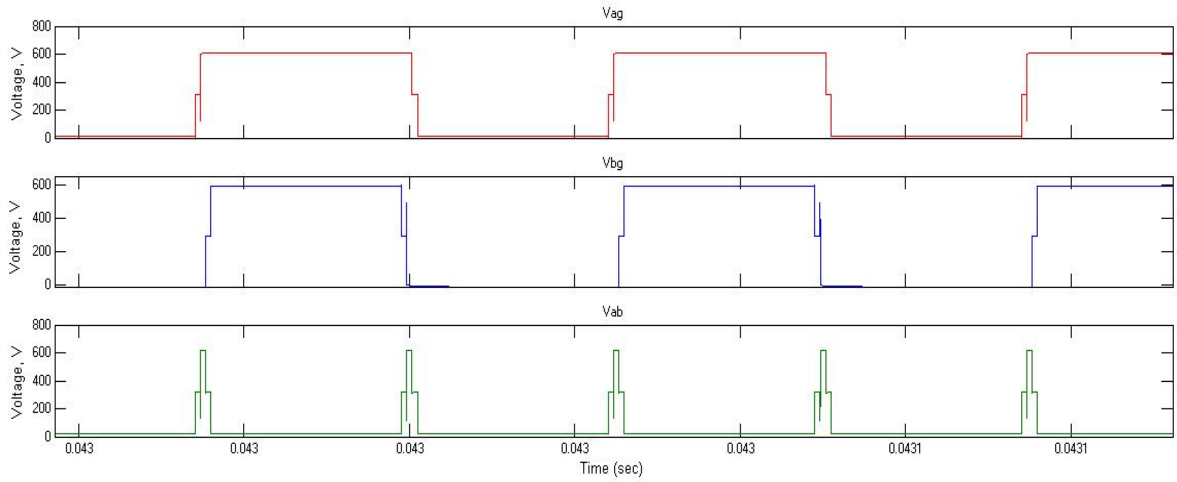

Figure 7. Three level output voltages of converter

The output voltage converter, V_0 is equal to 600V appeared across the load resistor shown in Fig.7. Whereas, the voltage ripples are very small in amplitude due to capacitors across the load resistor.

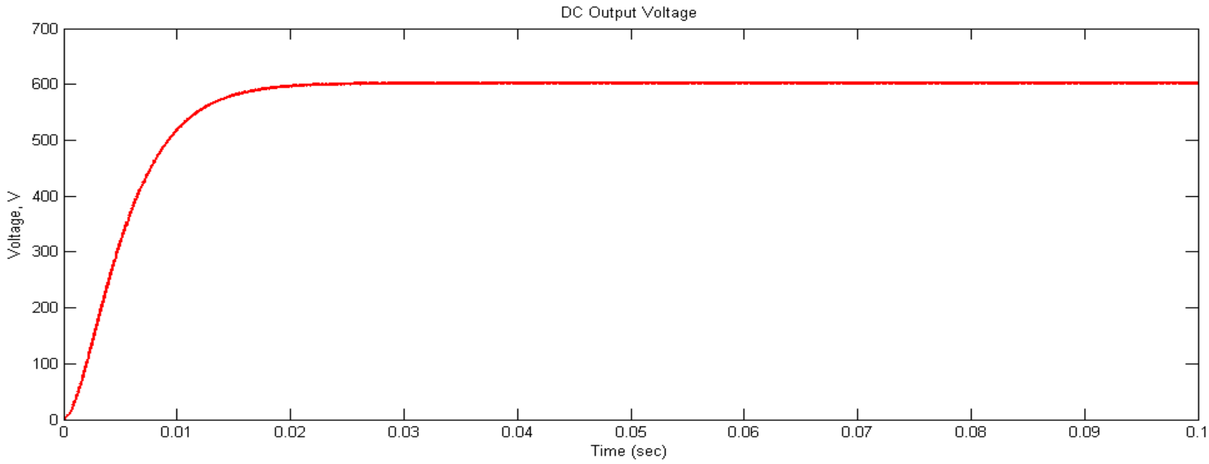

Figure 8. Output voltage of high gain boost converter

From the graphical analysis, the output power is 858W, the efficiency is nearer to 82% and the efficiency at full load is 96.6% shown in Fig. 9. By comparing the presented converter with classical topologies, this converter has less switching losses with less ESR and well suited for automobile applications.

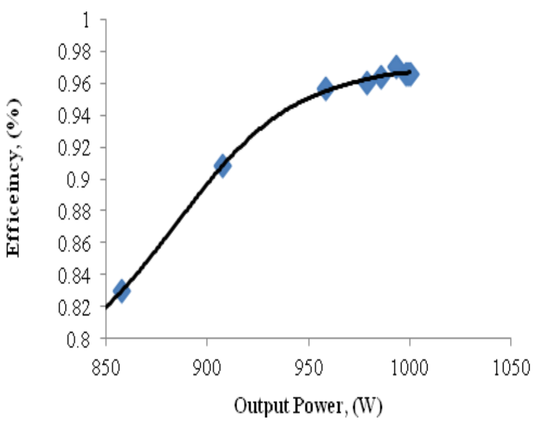

Figure 9. Output power versus Converter efficiency

VII. CONCLUSION

The non-isolated type converter is derived from neutral clamped inverter with excellent performance for electric vehicle applications. It is not only improving the converter's performance but also controls the duty ratio to minimum value. Here ripple current and voltage are derived to satisfy converter's requirement. The dynamic and steady state of both the filtering capacitors are balanced based by the PWM gating control technique. The major advantage with this converter, the voltage across the power switches is half of the output voltage. This converter is best for fuel cell based electric vehicle. The performance of the presented converter will be studied with respect to closed loop control in future.

REFERENCES

[1] X. Yu, M. R. Starke, L. M. Tolbert, and B. Ozpineci, "Fuel cell power conditioning for electric power applications : a summary," *IET Electr. Power Appl.*, vol. 1, no. 5, pp. 643–656, 2007.

[2] Q. Zhao and F. C. Lee, "High-efficiency, high step-up dc-dc converters," *IEEE Trans. Power Electron.*, vol. 18, no. 1 I, pp. 65–73, 2003.

[3] G. Vitale, "DC / DC Converter for HEVs and Resonant Active Clamping Technique."

[4] Y. Zhang, J. T. Sun, and Y. F. Wang, "Hybrid boost three-level DC-DC converter with high voltage gain for photovoltaic generation systems," *IEEE Trans. Power Electron.*, vol. 28, no. 8, pp. 3659–3664, 2013.

[5] P. Schuhmann, C. Graf, and K. a. Friedrich, "Modeling and Simulation of a PEM Fuel Cell System for Aircraft Applications P.Schumann," *ECS Trans.*, vol. 12, no. 1, pp. 651–661, 2008.

[6] A. Benrabah, F. Khoucha, O. Herizi, M. Benbouzid, A. Benrabah, F. Khoucha, O. Herizi, M. Benbouzid, and A. Kheloui, "FC / Battery Power Management for Electric Vehicle Based Interleaved DC-DC Boost Converter Topology To cite this version : FC / Battery Power Management for Electric Vehicle Based Interleaved dc-," 2014.

[7] E. Schaltz, A. Khaligh, and P. O. Rasmussen, "Influence of battery/ultracapacitor energy-storage sizing on battery lifetime in a fuel cell hybrid electric vehicle," *IEEE Trans. Veh. Technol.*, vol. 58, no. 8, pp. 3882–3891, 2009.

[8] S. K. Changchien, T. J. Liang, J. F. Chen, and L. S. Yang, "Novel high step-up DCDC converter for fuel cell energy conversion system," *IEEE Trans. Ind. Electron.*, vol. 57, no. 6, pp. 2007–2017, 2010.

[9] H. Wu and X. He, "Single phase three-level power factor correction circuit with passive lossless snubber," *IEEE Trans. Power Electron.*, vol. 17, no. 6, pp. 946–953, 2002.

[10] O. Hegazy, J. Van Mierlo, and P. Lataire, "Analysis, modeling, and implementation of a multidevice interleaved DC/DC converter for fuel cell hybrid electric vehicles," *IEEE Trans. Power Electron.*, vol. 27, no. 11, pp. 4445–4458, 2012.

[11] R. Stala, "Application of balancing circuit for DC-link voltages balance in a single-phase diode-clamped inverter with two three-level legs," *IEEE Trans. Ind. Electron.*, vol. 58, no. 9, pp. 4185–4195, 2011.

[12] A. K. S. Bhat and F. Dong Tan, "A Unified Approach to Characterization of PWM and Quasi-PWM

Switching Converters: Topological Constraints, Classification, and Synthesis," *IEEE Trans. Power Electron.*, vol. 6, no. 4, pp. 719–726, 1991.

[13] C. T. Pan and C. M. Lai, "A high-efficiency high step-up converter with low switch voltage stress for fuel-cell system applications," *IEEE Trans. Ind. Electron.*, vol. 57, no. 6, pp. 1998–2006, 2010.

[14] A. Ajami, H. Ardi, and A. Farakhor, "A Novel High Step-up DC/DC Converter Based on Integrating Coupled Inductor and Switched-Capacitor Techniques for Renewable Energy Applications," *IEEE Trans. Power Electron.*, vol. 30, no. 8, pp. 4255–4263, 2015.